ISSN 1063-7826, Semiconductors, 2016, Vol. 50, No. 7, pp. 951–956. © Pleiades Publishing, Ltd., 2016.
Original Russian Text © I.S. Kotousova, S.P. Lebedev, A.A. Lebedev, 2016, published in Fizika i Tekhnika Poluprovodnikov, 2016, Vol. 50, No. 7, pp. 967–972.

CARBON SYSTEMS

Electron-Diffraction Study of Graphene-Film Growth Stages during the Thermal Destruction of 6*H*-SiC (000$\bar{1}$) in Vacuum

I. S. Kotousova[a], S. P. Lebedev[a, b], and A. A. Lebedev[a, b]*

[a] *Ioffe Physical–Technical Institute, Russian Academy of Sciences, ul. Politekhnicheskaya 26, St. Petersburg, 194021 Russia*
[b] *National Research University of Information Technologies, Mechanics and Optics, pr. Kronverkskii 49, St. Petersburg, 197101 Russia*
** e-mail: shura.lebe@mail.ioffe.ru*

Submitted December 28, 2015; accepted for publication January 11, 2016

Abstract—The structure of graphene layers grown by sublimation on a 6*H*-SiC (000$\bar{1}$) substrate surface is studied by electron diffraction depending on the sublimation temperature and substrate-surface pretreatment method. It is shown that the use of polishing sublimation etching of the substrate before thermal destruction at a temperature of 1350°C on the substrate surface results in the formation of single-crystal graphene domains with graphene-lattice rotation by 30° with respect to the SiC lattice and a small fraction of amorphous domains. An increase in the temperature to 1500°C leads to the partial formation of a polycrystalline graphene phase with turbostratic structure while retaining the preferred orientation of graphene crystallites as at 1350°C. The use of pregrowth annealing before thermal destruction makes it possible to grow a graphene film with a more ordered and homogeneous structure without inclusions of amorphous and polycrystalline components. The preferred orientation of graphene domains in the film remains unchanged.

DOI: 10.1134/S1063782616070083

1. INTRODUCTION

As is known, graphene, for the discovery of which Andrei Geim and Konstantin Novoselov, scientists of Russian origin, were awarded the 2010 Nobel Prize in Physics, represents two-dimensional carbon layers. Graphene has certain advantages which make it possible to consider it as a material for developing devices which implement the principles of ballistic electronics, spintronics, optoelectronics, nanoplasmonics, and other promising alternatives to conventional semiconductor electronics. There are several methods for producing graphene: the "exfoliation" of graphite, growth on a SiC surface by sublimation, chemical deposition onto a metal surface, and others.

The best structural quality is inherent to graphene layers obtained by exfoliation. However, these layers have micrometer sizes and irregular geometrical shape. This makes them unsuitable for use in industry.

In second place in terms of structure quality and electrical parameters are graphene films grown on the surface of silicon carbide. Such films grown on SiC substrates 3 inches in diameter exhibit uniform parameters over the whole wafer area.

Such wafers can be used in a standard manufacturing line for fabricating semiconductor devices. An additional advantage of this technology is the possibility of obtaining a graphene film on a SiC semi-insulating substrate, which eliminates the need to transfer the grown film onto an insulator substrate, as takes place during growth on Mo and other metals.

Among the disadvantages of this technology are the formation of graphene films of a nonuniform thickness and the presence of structural defects. To optimize the technology, it is necessary to study the process of graphene-film nucleation and subsequent formation during silicon carbide thermal destruction.

Over the last few years, an extremely large number of works have been devoted to the study of the epitaxial growth of graphene films, involving such methods as low-energy electron diffraction, surface X-ray diffraction using synchrotron-radiation sources, Raman and photoelectron spectroscopy, scanning tunneling microscopy, atomic-force and transmission microscopy, and others.

This paper is devoted to the diffraction study of the structure of graphene layers formed on one of the polar faces of silicon carbide 6*H*-SiC (000$\bar{1}$) (the so-called C-face) due to its vacuum annealing at various temperatures and with various surface states of the face under study using the reflection electron-diffraction method.

The reflection electron-diffraction method [1, 2] (in the modified form, the reflection high-energy electron diffraction (RHEED) method is used along with the low-energy electron-diffraction (LEED) method to determine the structure of a single-crystal

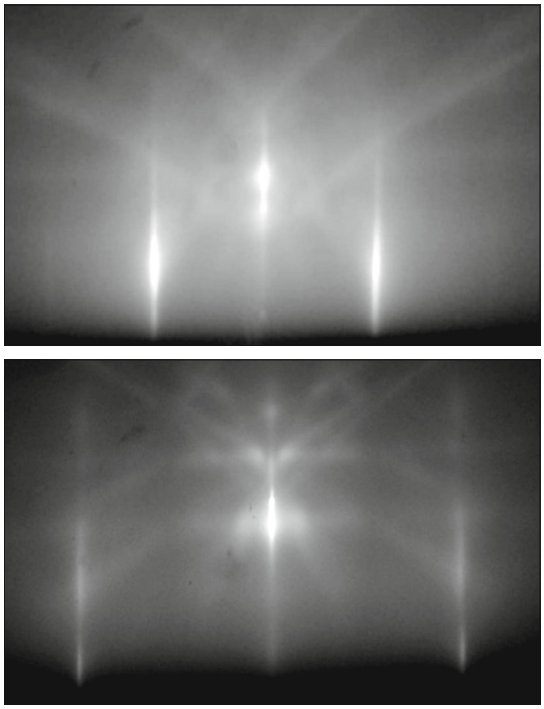

Fig. 1. Electron-diffraction patterns of the 6*H*-SiC initial substrate surface, measured in the (a) $[\bar{1}2\bar{1}0]$ and (b) $[\bar{1}100]$ azimuths.

surface, to study the relative orientation in the case of the contact of different phases and the formation of transition structures. The RHEED method has a number of advantages over the LEED method, i.e., RHEED diffraction patterns allow estimation of the structure quality of a single-crystal surface and its morphology, unlike LEED patterns; furthermore, they make it possible to differentiate reflections from two-dimensional and three-dimensional structures and to determine interplanar distances in a lattice with higher accuracy.

2. SAMPLES AND EXPERIMENTAL

The samples for structural studies were semi-insulating (resistivity is $> 10^5$ Ω cm) 6*H*-SiC substrates (CREE Co.) with a mechanically polished C-face surface, used in the technology of the fabrication of semiconductor devices. Graphene layers were synthesized by thermal decomposition of the 6*H*-SiC $(000\bar{1})$ surface in a vacuum sublimation epitaxy system using the technology proposed in [3] at two silicon sublimation temperatures, 1350 and 1500°C, for 5 min.

Before graphene synthesis, scratches and other defects which always remain after the mechanical polishing of a substrate surface were preliminarily removed. In the first stage, to remove the mechanically damaged surface layer of the substrate, polishing sublimation etching [3] was used; later, this was replaced by the method of pregrowth substrate annealing [4] in a closed cell of the growth chamber. As atomic-force microscopy showed [3, 5], both these pretreatment methods lead to removal of the mechanically damaged surface layer and the formation of a surface shaped as extended terraces ~250 Å wide and steps with a height equal to the SiC unit-cell parameter. However, in contrast to the initially applied method used in [3], the use of pregrowth annealing [4, 5] provides atomically smooth terrace surfaces.

Diffraction patterns of the sample surface were measured using an EMR-100 electron diffractometer at an accelerating voltage of 50 kV at the Analytical chemistry department of the Saint Petersburg State Technological Institute.

Electron-diffraction patterns of the 6*H*-SiC $(000\bar{1})$ surface were measured in the direction of a grazing electron beam incident on the surface parallel to the crystallographic directions with low indices in the basal plane and in the angular range between these directions which were fixed using a goniometer.

3. RESULTS AND DISCUSSION

The typical reflection electron-diffraction patterns of the sample surfaces and the indexing results are shown in Figs. 1a–4a and 1b–4b (in the $[\bar{1}2\bar{1}0]$ and $[\bar{1}100]$ azimuths with respect to the substrate, respectively) and in Fig. 2c–4c for deviations from these azimuths.

The electron-diffraction patterns in Fig. 1 show the initial substrate-surface state, and Figs. 2–4 show the surface state after thermal destruction.

The electron diffraction patterns of the SiC substrate surface (Figs. 1a and 1b) consist of vertical rod-like reflections characteristic of single crystals, and a well developed system of Kikuchi lines, which indicates a rather high degree of perfection of the substrate surface structure in the initial state.

In the electron-diffraction patterns of the surface of the sample not subjected to pregrowth annealing, the Kikuchi lines disappeared after thermal destruction at a temperature of 1350°C for 5 min (Figs. 2a and 2b) (indicating structural damage in the SiC surface layer); however, new "single-crystal" reflections appeared (denoted by *G* in the electron-diffraction patterns).

For example, in the electron-diffraction pattern (Fig. 2a) measured in the $[\bar{1}2\bar{1}0]$ azimuth, being the (010) reciprocal lattice section, reflections corresponding to 11.*l* graphite reflections appeared; in the electron-diffraction pattern (Fig. 2b) measured in the $[\bar{1}100]$ azimuth, reflections corresponding to the 10.*l* graphite reflections appeared in the $(\bar{1}10)$ section of the SiC reciprocal lattice. The 11.*l* graphite reflections in the (010) section of the SiC reciprocal lattice and

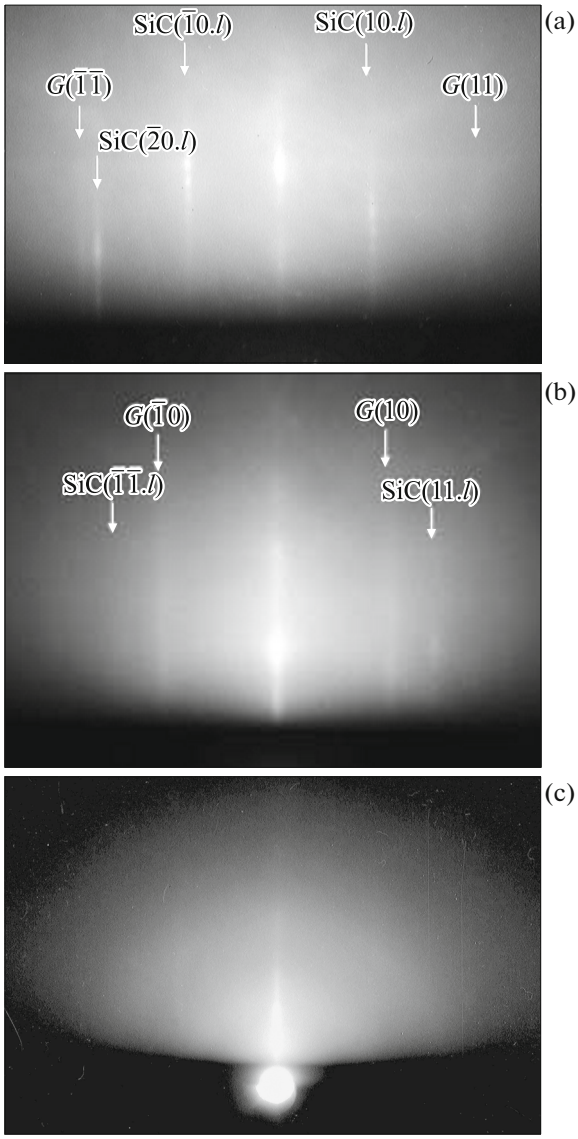

Fig. 2. Electron-diffraction patterns of the 6*H*-SiC surface after thermal destruction at $T = 1350$°C for 5 min, without pregrowth annealing, measured in the (a) $[\bar{1}2\bar{1}0]$ and (b) $[\bar{1}100]$ azimuths, and (c) with a deviation from these azimuths.

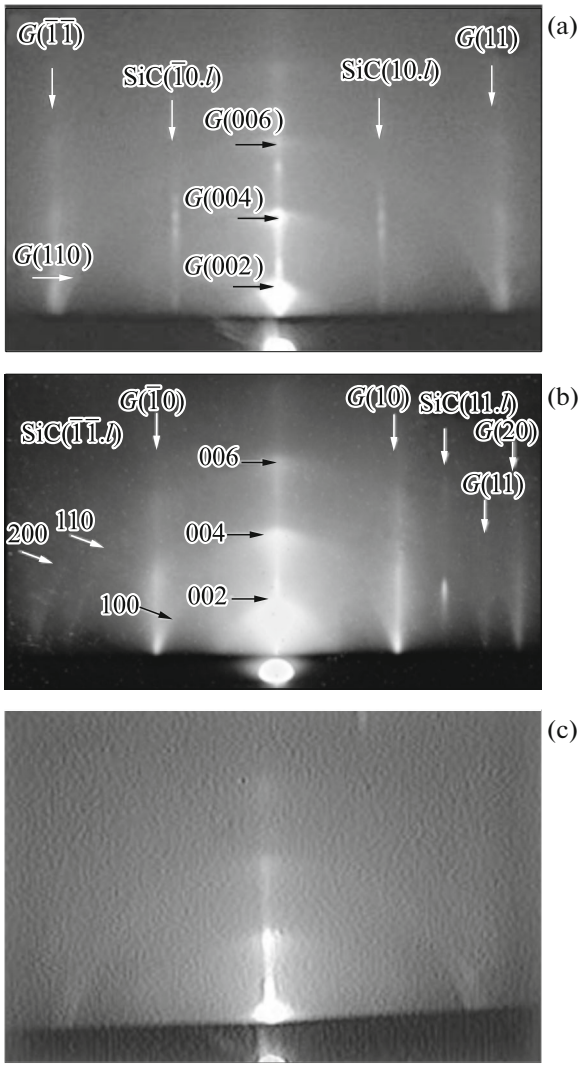

Fig. 3. Electron-diffraction patterns of the 6*H*-SiC surface after thermal destruction at $T = 1500$°C for 5 min, without pregrowth annealing, measured (a) in the $[\bar{1}2\bar{1}0]$ azimuth, (b) near the $[\bar{1}100]$ azimuth (b), and (c) with a deviation from these azimuths.

10.*l* in the $(\bar{1}10)$ section can appear only in the case of graphite-lattice rotation by 30° with respect to the SiC lattice. We note the reflections that appeared in the electron-diffraction patterns after thermal destruction are shaped as continuous rods with a uniform intensity over the rod height, in contrast to the rodlike reflections of SiC characterized by either nonuniform intensities over height (Fig. 1a) or by their discontinuity (Fig. 1b). The observed diffraction pattern of SiC (Figs. 1a, 1b) is typical of the case of RHEED of a single crystal surface with a rather high degree of perfection, according to electron-diffraction theory and practice [1, 2]. At the same time, according to the Laue theory of diffraction by two-dimensional crystals, the reflections observed in the electron-diffraction patterns in Figs. 1a and 1b, shaped as continuous rods, should be attributed to *hk* reflections from single graphite layers, i.e., graphene.

Thus, the diffraction patterns of the sample surface annealed at 1350°C, measured in the $[\bar{1}2\bar{1}0]$ and $[\bar{1}100]$ azimuths, indicate graphene formation on silicon carbide with graphene-lattice rotation by 30° with respect to the SiC lattice.

The electron-diffraction patterns of the sample surface with deviations from the $[\bar{1}2\bar{1}0]$ and $[\bar{1}100]$ directions allowed us to detect that a diffraction pattern consisting of diffuse rings (Fig. 2c) appears near

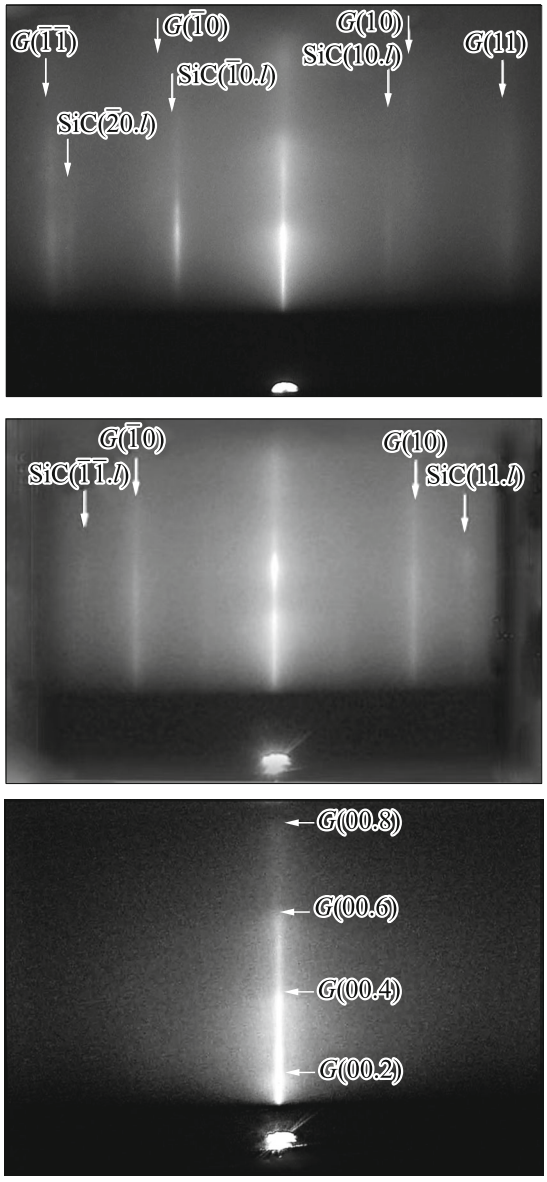

Fig. 4. Electron-diffraction patterns of the 6*H*-SiC surface after thermal destruction at $T = 1500$°C for 5 min, with pregrowth annealing, measured (a) near the $[\bar{1}2\bar{1}0]$ azimuth, (b) in the $[\bar{1}100]$ azimuth, and (c) with a deviation from these azimuths.

$[\bar{1}100]$ (with a deviation from this azimuth by 2°–3°). A similar pattern sometimes appeared for some individual surface areas of the sample under study, without any azimuthal regularity. Analysis of the electron-diffraction patterns in Fig. 2c showed that the diffuse rings can be related to the (10.0) and (11.0) reflections of amorphous graphene.

The general understanding of the structure of this sample, revealed by reflection electron diffraction, is consistent with the LEED results for the structure of graphene layers formed at early stages during 4*H*- and 6*H*-SiC $(000\bar{1})$ surface thermal destruction in high vacuum [6–8].

The electron-diffraction patterns of the sample obtained by thermal destruction of the silicon-carbide surface at a temperature of 1500°C for 5 min (which, as the previous sample, was not subjected to pregrowth annealing before thermal destruction of the silicon carbide), are shown in Figs. 3a–3c. We can see that an increase in the sublimation temperature led to a significant change in the diffraction patterns.

In the electron-diffraction patterns of the sample surfaces, measured in $[\bar{1}2\bar{1}0]$ and $[\bar{1}100]$ azimuths (Fig. 3a and 3b,), in contrast to the electron-diffraction patterns in Figs. 2a and 2b, the rodlike reflections appeared after annealing, which correspond to graphite, are not uniform in height, but exhibit periodic intensity changes over rod height. Furthermore, the electron-diffraction patterns in Fig. 3a and 3b exhibit diffuse reflections at the so-called specular reflection (in contrast to the electron-diffraction patterns in Figs. 2a and 2b). The diffuse reflections that appeared (Figs. 3a and 3b) correspond to the 002, 004, and 006 graphite reflections, but with an interlayer distance excessive for graphite: for 002, $d_{002} = 3.43$ Å instead of 3.354 Å characteristic of graphite.

The next difference between the electron-diffraction patterns in Figs. 3a and 3b and Figs. 2a and 2b is the presence of weak reflections characteristic of polycrystals in Figs. 3a and 3b and their absence in Figs. 2a and 2b. These reflections correspond to the 100, 110, and 200 graphite reflections, but with decreased interplanar distances d_{100} and d_{110} in comparison with graphite, 2.12 and 1.225 Å instead of 2.13 and 1.232 Å characteristic of graphite. The size of the coherent-scattering regions (CSRs) of the polycrystalline component in the graphene film formed at a temperature of 1500°C is ~100 Å.

Thus, the detection of a fine-grained polycrystalline component with a structure similar to graphite, but with excessive d_{002} and undersized d_{110}, in the film under study, and periodic intensity modulations in rodlike reflections *hk* corresponding to graphene reflections in the diffraction patterns, suggest that the film under study contains some regions with two-dimensional turbostratic structure [9, 10]. In this structure, parallel graphene layers are in a random azimuthal orientation with respect to each other.

Measurements of the electron-diffraction patterns with a deviation from the $[\bar{1}2\bar{1}0]$ and $[\bar{1}100]$ directions also showed the presence of polycrystalline components in certain graphene-film regions (Fig. 3c).

We note that analysis of the specular reflection showed that different interlayer distances correspond to individual 00*l* reflections often in the absence of

"polycrystalline" reflections in the electron-diffraction patterns. It was found that the interlayer distance in the first layer is (3.2 ± 0.05) Å; in the second layer in the electron-diffraction patterns of various sample areas, it is from 3.5 to 3.7 Å; and the interlayer distance of subsequent layers is (3.41 ± 0.01) Å.

A comparison of the electron-diffraction patterns of samples grown at 1300 and 1500°C on substrates not subjected to pregrowth annealing (Figs. 2a and 2b and Figs. 3a and 3b) allows us to complement the above distinctive features of the diffraction patterns in Figs. 3a and 3b by the appearance of weak rodlike 10 and 11 reflections of graphene in the (010) and ($\bar{1}$10) reciprocal-lattice sections, respectively. This phenomenon suggests that a certain fraction of domains with orientation coinciding with the substrate orientation appears in the film grown at 1500°C, in addition to the dominant rotation of graphene domains by angle of 30° with respect to the substrate, observed in the sample annealed at 1350°C.

Figures 4a–4c show the electron-diffraction patterns of the sample obtained, as the previous one, as a result of thermal destruction at a temperature of 1500°C for 5 min, but subjected to pregrowth annealing before thermal destruction.

As in the electron-diffraction patterns of the sample without pregrowth annealing (Fig. 3), the electron-diffraction patterns in Fig. 4 contain 00*l* reflections at the specular reflection corresponding to graphite with interlayer distances excessive for graphite, but without accompanying reflections from the polycrystalline structure as in Fig. 3; furthermore, 00*l* reflections in the electron-diffraction patterns in Fig. 4 have a less distinct diffuse nature that in those of the samples without pregrowth annealing. The absence of rings characteristic of polycrystals and the less distinct diffuse nature of 00*l* reflections in the electron-diffraction patterns of the sample subjected to pregrowth annealing before synthesizing graphene layers at a temperature of 1500°C, indicate the more ordered structure of the graphene film in comparison with the case of film formation on the sample without pregrowth annealing.

The diffraction patterns in Fig. 4 suggest that single graphene layers are associated into rather extended stacks [10]. The calculated interlayer distance in graphene film stacks, except for the first layer, is (3.40 ± 0.01) Å which is slightly smaller than in the turbostratic structure. For the first layer, the interlayer distance is only (3.2 ± 0.05) Å. To our knowledge, there are several papers with experimentally determined interlayer distances in the graphene film grown on the C-face. Using X-ray diffraction method, the interlayer distance in the film samples on the 4*H*-SiC substrate, grown in high vacuum, was determined in [10] as 3.368 Å; in [11], simultaneously two values were found in one sample, 3.37 and 3.42 Å, also grown on 4*H* polytype, but in an Ar atmosphere. Using high-resolution transmission electron microscopy, the interlayer distance in the graphene samples on the 6*H*-SiC substrate grown in vacuum was determined in [12] as 3.39 Å; in [13], for samples grown on the 4*H* polytype, it was determined as 3.40 Å [14].

Thus, the interlayer distance of 3.40 Å calculated based on measurements of electron-diffraction patterns of the 6*H*-SiC sample after thermal destruction at 1500°C is in agreement with the above results.

The increase in the interlayer distance in the graphene film grown on the C face of silicon carbide is associated with a specific film-growth mechanism, when each new layer is displaced by a certain angle with respect to the previous one [15–17], in contrast to chaotic rotations or displacements of layers forming stacks of the turbostratic structure. As a result, the multilayer film gains quasi-ordered packing while retaining the preferred graphene orientation with its lattice rotation of 30° with respect to the substrate lattice.

4. CONCLUSIONS

The electron-diffraction study of layers synthesized on the 6*H*-SiC (000$\bar{1}$) substrate surface by thermal decomposition in vacuum showed that the use of polishing sublimation etching of the substrate before thermal destruction at the early stage of layer formation (at a temperature of 1350°C) leads to the formation of domains of single-crystal graphene with its lattice rotated by 30° with respect to the SiC lattice and a small fraction of amorphous domains. It was shown that an increase in the temperature to 1500°C results in partial formation of the polycrystalline graphene phase with turbostratic structure while retaining the preferred graphene orientation, as in the case of 1350°C.

Due to the use of the pregrowth annealing operation before thermal destruction, the synthesized graphene film gains a more ordered and homogeneous structure.

ACKNOWLEDGMENTS

We are grateful to V.P. Rubets and V.V. Antipov (Saint Petersburg State Technological Institute) for the provided opportunity to perform electron-diffraction studies.

REFERENCES

1. Z. G. Pinsker, Electron Diffraction (Akad. Nauk SSSR, Moscow, 1949) [in Russian].
2. L. A. Zhukova and M. A. Gurevich, *Electron Diffraction Analysis of Surface Layers and Films of Semiconductor Materials* (Metallurgiya, Moscow, 1971) [in Russian].

3. A. A. Lebedev, I. S. Kotousova, A. A. Lavrent'ev, S. P. Lebedev, I. V. Makarenko, V. N. Petrov, and A. N. Titkov, Phys. Solid State **51**, 829 (2009).
4. S. P. Lebedev, V. N. Petrov, A. A. Lavrent'ev, P. A. Dement'ev, A. A. Lebedev, and A. N. Titkov, Mater. Sci. Forum **679**, 437 (2011).
5. A. A. Lebedev, N. V. Agrinskaya, S. P. Lebedev, M. G. Mynbaeva, V. N. Petrov, A. N. Smirnov, A. M. Strel'chuk, A. N. Titkov, and D. V. Shamshur, Semiconductors **45**, 623 (2011).
6. C. C. Mathieu, N. Barrett, J. Rault, Y. Y. Mi, B. Zhang, W. A. de Heer, C. Berger, E. H. Conrad, and O. Renault, Phys. Rev. B **83**, 235436 (2011).
7. P. Avouris and C. Dimitrakopoulos, Mater. Today **15**, 86 (2012).
8. N. Srivastava, G. He, R. M. Feenstra, and P. J. Fisher, Phys. Rev. B **82**, 235406 (2010).
9. R. E. Franklin, Acta Crystallogr. **4**, 253 (1951).
10. A. V. Kurdyumov and A. N. Pilyankevich, *Phase Transformations in Carbon and Boron Nitride* (Nauk. Dumka, Kiev, 1979) [in Russian].
11. J. Hass, F. Varchon, J. E. Millan-Otoya, M. Sprinkle, N. Sharma, W. A. de Heer, C. Berger, P. N. First, L. Magaud, and E. H. Conrad, Phys. Rev. Lett. **100**, 125504 (2008).
12. T. G. Mendes-de-Sa, A. M. B. Goncalves, M. J. S. Matos, P. M. Coelho, R. Magalhaes-Paniago, and R. G. Lacerda, Nanotechnology **23**, 475602 (2012).
13. A. A. Lebedev, N. V. Agrinskaya, V. A. Beresovets, V. I. Kozub, S. P. Lebedev, and A. A. Sitnikova, arXiv:1212.4272 (2012).
14. J. Borysiuk, J. Soltys, and J. Piechota, J. Appl. Phys. **109**, 093523 (2011).
15. M. Sprinkle, J. Hicks, A. Tejeda, A. Taleb-Ibrahimi, P. le Févre, F. Bertran, H. Tinkey, M. C. Clark, P. Soukiassian, D. Martinotti, J. Hass, and E. H. Conrad, J. Phys. D: Appl. Phys. **43**, 374006 (2010).
16. A. Tejeda, A. Taleb-Ibrahimi, W. de Heer, C. Berger, and E. H. Conrad, New J. Phys. **14**, 125007 (2012).
17. J. Kuroki, W. Norimatsu, and M. Kusunoki, Surf. Sci. Nanotechnol. **10**, 396 (2012).

Translated by A. Kazantsev